Fragmentation of Actin Filaments†

Albrecht Wegner* and Paula Savko

ABSTRACT: The kinetics of actin polymerization were analyzed by taking into account nucleation, elongation, and spontaneous fragmentation of filaments. Polymerization curves measured in the presence of potassium (40 mM) were found to be in good agreement with curves calculated for the assumption that nucleation and elongation but no fragmentation reactions occur. Polymerization curves measured in the presence of calcium (1.8 mM) or magnesium (0.6 mM $MgCl_2$ and 0.5 mM EGTA) could only be simulated by calculated curves when spontaneous fragmentation was assumed to occur in addition to nucleation and elongation. The experiments reported in this study suggest that even in the absence of ultrasonication or shear forces actin filaments may break spontaneously and that the extent of fragmentation depends strongly on the experimental conditions. Spontaneous fragmentation changes the shape of the polymerization curves significantly. When fragmentation of filaments takes place, a relatively long lag phase of polymerization is observed that is followed by a strongly increasing polymerization rate to reach the final constant value quickly. On the other hand, when filaments are formed exclusively by nucleation, the polymerization curves approach the final constant value slowly after a relatively short initial lag phase.

End-to-end association of actin filaments has been reported by Nakaoka & Kasai (1969) and by Kondo & Ishiwata (1976). The reverse reaction, namely, spontaneous fragmentation of filaments in the absence of ultrasonication or shear forces, has neither been demonstrated nor been excluded. Investigations on the spontaneous fragmentation of actin filaments are necessary for an understanding of the action of a number of proteins or other molecules that have been reported to cause long actin filaments to be converted into short actin filament fragments [e.g., cytochalasin (Brenner & Korn, 1979; MacLean-Fletcher & Pollard, 1980) or fragmin (Hasegawa et al., 1980)]. The action of these filament-shortening molecules can be explained in two ways: (i) Actin filaments break spontaneously, and the fragments are prevented from end-to-end reassociation by blocking of one end of the filaments by the filament-shortening molecules. (ii) The filament-shortening molecules disrupt actin filaments.

Whereas end-to-end association of actin filaments can be demonstrated by electron microscopy (Nakaoka & Kasai, 1969; Kondo & Ishiwata, 1976), an analogous direct visualization of spontaneous fragmentation is impossible. We, therefore, studied the problem of fragmentation by analyzing the polymerization kinetics of actin.

Materials and Methods

(*a*) *Preparation of Actin.* Actin was prepared from rabbit skeletal muscle according to the method of Rees & Young (1967) with the alteration that the protein was chromatographed on Bio-Gel P-150 and protected against denaturation by modification at cysteine-373 with *N*-ethylmaleimide (Lusty & Fasold, 1969). The actin concentration was determined photometrically at 290 nm by using an extinction coefficient of 24900 M^{-1} cm^{-1} (Wegner, 1976).

(*b*) *Light Scattering.* Actin polymerization was initiated by mixing 1 volume of a buffer containing salt with 2 volumes of a dialyzed monomeric actin solution. Both the salt buffers and the dialysis buffers contained 500 μM ATP, 5 mM tri-ethanolamine hydrochloric acid (pH 7.5), and 6 mM NaN_3. The components by which the buffers were different are given in Table I. Before mixing in light-scattering cells, all solutions were centrifuged for 1 h at 150000*g* in order to remove dust and actin filaments.

The light-scattering intensity $R(\vartheta)$ of long polydisperse rodlike protein aggregates such as actin filaments has been shown to be given by (Casassa, 1955)

$$R(\vartheta) = K\left(\frac{\lambda}{4 \sin (\vartheta/2)}\right)\left(\frac{M}{L}\right)C^* \qquad (1)$$

ϑ is the observation angle, K is an optical constant, C^* is the concentration of actin filament subunits, λ is the wavelength of light in the solvent, M is the molecular weight of a filament subunit, and L is the length per filament subunit. Equation 1 has been derived for rodlike particles, the length of which exceeds $\lambda/[4\pi \sin (\vartheta/2)]$ ($\sim$50 nm) and the diameter of which is smaller than $\lambda/[4\pi \sin (\vartheta/2)]$. Short filaments, the length of which is in the range of 50 nm or below, contribute less light-scattering intensity per subunit than long filaments. Studies by electron microscopy and by light scattering have shown that the bulk of actin filaments is considerably longer than 50 nm (Kawamura & Maruyama, 1970; Wegner & Engel, 1975). It can be demonstrated that the scattering intensity of monomeric actin is so small compared to the scattering intensity of filaments that no correction needs to be applied for scattering by monomers.

All light-scattering measurements were performed at 546 nm under a 90° observation angle by using a fluorometer (Farrand Mark I). The photometer was calibrated by the light-scattering intensity of solutions containing a known concentration of polymerized actin. The light-scattering intensity of the cells containing pure buffer was subtracted from the total scattering intensity.

Results

(*a*) *Theory.* In this section a kinetic model for formation of actin filaments will be set up that takes into account nucleation by consecutive association of monomers as well as spontaneous fragmentation of filaments. In the latter part of this section approximations will be introduced that permit mathematical handling of the kinetic rate equations. The experimental data and their interpretation will be presented in the next section.

† From the Department of Biophysical Chemistry, Biozentrum, CH-4056 Basel, Switzerland. *Received June 22, 1981.*

* Address correspondence to this author at the Institut fuer Physiologische Chemie I, Ruhr-Universitaet Bochum, Postfach 102148, D-4630 Bochum, West Germany. Recipient of a Heisenberg-Fellowship from the Deutsche Forschungsgemeinschaft.

0006-2960/82/0421-1909$01.25/0

Table I: Experimental Conditions and Determined Parameters

main cation	potassium	calcium	magnesium
buffer for dialysis of actin	10 μM $MgCl_2$	0.2 mM $CaCl_2$	10 μM $MgCl_2$
salt buffer	120 mM KCl, 10 μM $MgCl_2$	5 mM $CaCl_2$	1.78 mM $MgCl_2$, 1.5 mM EGTA
experimental conditions	40 mM KCl, 10 μM $MgCl_2$	1.8 mM $CaCl_2$	0.6 mM $MgCl_2$, 0.5 mM EGTA
simplest mechanism of filament formation	fast monomer–trimer preequilibrium, no detectable fragmentation	fast monomer–tetramer preequilibrium, fragmentation	fast monomer–tetramer preequilibrium, fragmentation
critical monomer concentration $\bar{c}_1 = k'/k$	1.5 μM	2.0 μM	2.0 μM
$k'^2 \prod_{i=2}^{i=n} (k_i/k_i')$	$n = 3$, 6.6 M^{-2} s^{-2}	$n = 4$, 3.2×10^5 M^{-3} s^{-2}	$n = 4$, 1.9×10^5 M^{-3} s^{-2}
$k'k_{fr}$		2.5×10^{-9} s^{-2}	7.5×10^{-8} s^{-2}

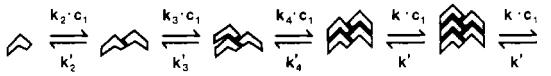

FIGURE 1: Illustration of a possible induced-fit nucleation and elongation reaction.

The rate constant for association of a monomer with another monomer is likely to be different from the rate constant for binding of a monomer to a filament end because of the different number of contacts with other subunits (Oosawa & Kasai, 1962) (Figure 1). Furthermore a cooperativity of nucleation may be attributed to the entropy of free subunits that is required to immobilize the subunits in the filament, as recently pointed out by Erickson & Pantaloni (1981). It is also conceivable that binding of a monomer to small aggregates depends on the size of the aggregates due to induced fit as displayed in Figure 1. Above a critical number n of subunits, the association and dissociation rate constants are assumed to be independent of the filament length because of the equivalence of the binding sites. The association or dissociation reaction has been shown experimentally to occur in a second-order or a first-order reaction, respectively (Pollard & Mooseker, 1981). The reactions and the corresponding rate constants are represented in Scheme I.

Actin polymerization may be more complicated than depicted in Scheme I. However, this study is limited to an explanation of available kinetic experimental data by a model that is as simple as possible.

Because of the complexity of the reaction scheme and of the long computer times needed for simulations, approximations will be introduced that permit simplification of the rate equations. The introduced approximations are essentially an extension of the treatment of Wegner & Engel (1975) to filament fragmentation.

After a brief initial phase of polymerization, changes in the concentration of short filaments contribute negligibly to changes in the total number concentration of filaments C. The limit between short and longer filaments has to be chosen so that the longer filaments comprise the bulk of the filaments:

$$\sum_{i=2}^{i=l} c_i \ll \sum_{j=l+1}^{\infty} c_j \tag{2}$$

where the polymerization degree l is the limit between short and longer filaments and c_i or c_j is the concentration of actin aggregates with i or j subunits, respectively. With this approximation the rate of filament formation is given by

$$\frac{dC}{dt} = \frac{d\sum_{j=l+1} c_j}{dt} + k_{fr} \sum_{j=l+1} j c_j = k c_1 c_l - k' c_{l+1} + k_{fr}(c_{tot} - c_1) \tag{3}$$

Scheme I[a]

$$2A \underset{k_2'}{\overset{k_2}{\rightleftharpoons}} A_2$$

$$A_2 + A \underset{k_3'}{\overset{k_3}{\rightleftharpoons}} A_3$$

$$\vdots$$

$$A_{n-1} + A \underset{k_n'}{\overset{k_n}{\rightleftharpoons}} A_n$$

$$A_n + A \underset{k'}{\overset{k}{\rightleftharpoons}} A_{n+1}$$

$$\vdots$$

$$A_p + A \underset{k'}{\overset{k}{\rightleftharpoons}} A_{p+1} \quad p \geq n$$

$$A_{p+q} \xrightarrow{k_{fr}} A_p + A_q$$

[a] A stands for an actin monomer or subunit.

The short filaments can be regarded as intermediates occurring in concentrations that are small compared to the concentration of longer filaments (eq 2). Therefore, for the short aggregates the steady-state approximation is applicable.

$$\frac{dc_i}{dt} = 0 \tag{4}$$

The long filaments are formed if the number of filaments is small compared to the number of monomers. Under this condition the monomer concentration changes only little during the time necessary to elongate a filament by one subunit. As a consequence of the slow change of the monomer concentration and of the equal rates of formation and consumption of aggregates with l and $l + 1$ subunits, the concentrations c_l and c_{l+1} are practically equal.

$$c_l = c_{l+1} \tag{5}$$

If the concentration of nuclei comprise a negligibly small part of the total concentration, the monomers are mainly consumed by elongation of filaments. Thus

$$\frac{dc_1}{dt} = -(k c_1 - k') C \tag{6}$$

For calculation of the time course of the monomer concentration, the polymer concentration C occurring in eq 6 has to be expressed by the monomer concentration. Combining the rate equations for the formation of nuclei (see above reaction scheme and eq 4) and for the formation of filaments (eq 3 and 5, thereby setting l equal to n), one can arrange the kinetic equations in a matrix representation (see matrix I) that permits calculation of the filament concentration C in terms of the monomer concentration c_1. One can easily show that the time

Matrix I

$$\begin{pmatrix} -(k_2' + k_3c_1) & k_3' & 0 & \cdots & 0 & 0 & 0 & 0 \\ k_3c_1 & -(k_3' + k_4c_1) & k_4' & \cdots & 0 & 0 & 0 & 0 \\ 0 & k_4c_1 & -(k_4' + k_5c_1) & \cdots & 0 & 0 & 0 & 0 \\ \vdots & \vdots & \vdots & & \vdots & \vdots & \vdots & \vdots \\ 0 & 0 & 0 & \cdots & -(k_{n-2}' + k_{n-1}c_1) & k_{n-1}' & 0 & 0 \\ 0 & 0 & 0 & \cdots & k_{n-1}c_1 & -(k_{n-1}' + k_nc_1) & k_n' & 0 \\ 0 & 0 & 0 & \cdots & 0 & k_nc_1 & -(k_n' + kc_1 - k') & 0 \\ 0 & 0 & 0 & \cdots & 0 & 0 & -(kc_1 - k') & 1 \end{pmatrix} \begin{pmatrix} c_2 \\ c_3 \\ c_4 \\ \vdots \\ c_{n-2} \\ c_{n-1} \\ c_n \\ \frac{dC}{dt} \end{pmatrix} = \begin{pmatrix} -k_2c_1^2 \\ 0 \\ 0 \\ \vdots \\ 0 \\ 0 \\ 0 \\ k_{fr}(c_{tot} - c_1) \end{pmatrix}$$

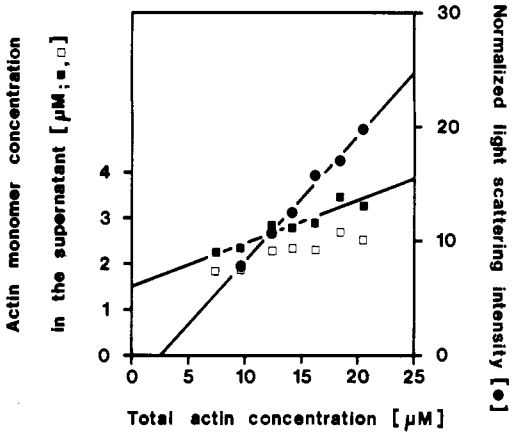

FIGURE 2: Determination of the critical monomer concentration of actin (40 mM KCl). (●) Light-scattering intensity normalized by the scattering intensity of 1 μM actin filament subunits vs. the total actin concentration. (■) Actin monomer concentration in the supernatant of centrifuged solutions vs. the total actin concentration. (□) Actin monomer concentration in the supernatant corrected for the nonpolymerizable actin vs. the total actin concentration.

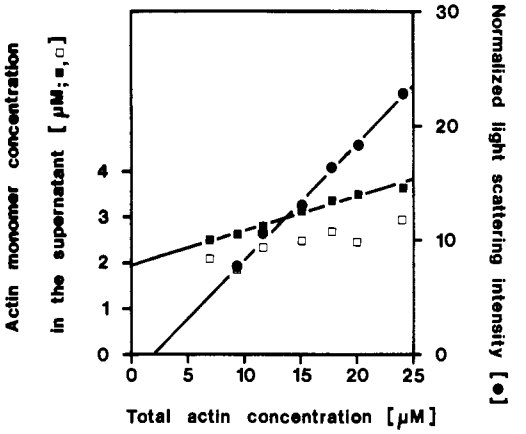

FIGURE 3: Determination of the critical monomer concentration of actin (1.8 mM $CaCl_2$). (●) Light-scattering intensity normalized by the scattering intensity of 1 μM actin filament subunits vs. the total actin concentration. (■) Actin monomer concentration in the supernatant of centrifuged solutions vs. the total actin concentration. (□) Actin monomer concentration in the supernatant corrected for the nonpolymerizable actin vs. the total actin concentration.

dependence of the monomer concentration c_1 is determined by $2n$ independent parameters, e.g., k'/k_2, k'/k_{fr}, k_i/k' ($3 \leq i \leq n$), k_i'/k' ($2 \leq i \leq n$), and k/k'. For this reason it is impossible to determine all $2n + 1$ rate constants by analyzing the time course of the monomer concentration. However, one can obtain an idea on the ratios between different rate constants and on the pathways leading to filament formation.

Of particular interest is the limiting case that the nuclei dissociate fast compared to the association of monomers with aggregates having n subunits ($k_2', \ldots, k_n' \gg kc_1$). Under this condition a fast preequilibrium is established between monomers and nuclei (see matrix I). The time course of filament formation reduces to

$$\frac{dC}{dt} = (kc_1 - k')c_1^n \prod_{i=2}^{i=n}(k_i/k_i') + k_{fr}(c_{tot} - c_1) \qquad (7)$$

Proof for the validity of the introduced approximations has been given by Wegner & Engel (1975) for the case that no fragmentation occurs. The approximated calculations have been shown to be in excellent agreement with a simulation of the full reaction scheme by numerical integration. The approximation presented in this section is also certainly valid as long as fragmentation is so slow that the short aggregates are formed mainly by consecutive association of monomers and not by fragmentation of filaments.

(*b*) *Experimental Data and Their Interpretation. Critical Monomer Concentration.* The critical monomer concentration was determined by extrapolation of the total concentration to zero light scattering intensity (Figures 2–4) (Oosawa & Kasai, 1962). As the extrapolated line intersects the abscissa near the origin, this method may not be accurate. Therefore, the critical concentration was determined by a second method. Monomers and filaments were separated by centrifugation

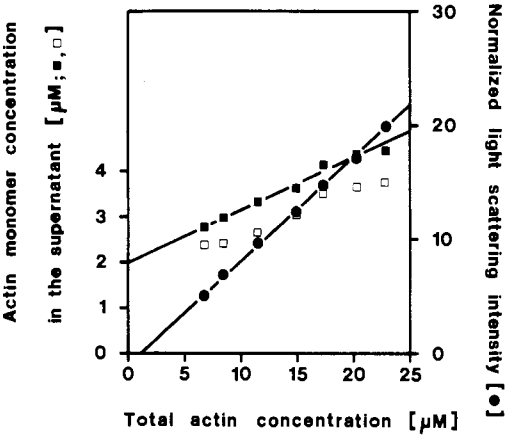

FIGURE 4: Determination of the critical monomer concentration of actin (0.6 mM $MgCl_2$ and 0.5 mM EGTA). (●) Light-scattering intensity normalized by the scattering intensity of 1 μM actin filament subunits vs. the total actin concentration. (■) Actin monomer concentration in the supernatant of centrifuged solutions vs. the total actin concentration. (□) Actin monomer concentration in the supernatant corrected for the nonpolymerizable actin vs. the total actin concentration.

(150000*g*, 1 h), and the monomer concentration was measured in the supernatants. The results are summarized in Figures 2–4. The monomer concentration was found to increase with increasing total actin concentration. The polymerizability of actin in the supernatant was tested by adjusting the salt concentrations to conditions optimal for polymerization, namely, 1 mM $MgCl_2$ and 100 mM KCl. The monomer concentrations corrected by the unpolymerized actin concentrations are depicted in Figures 2–4. Under optimal conditions the critical concentration is in the range 0.1–0.2 μM (Walsh & Wegner, 1980). The observed dependence of the monomer

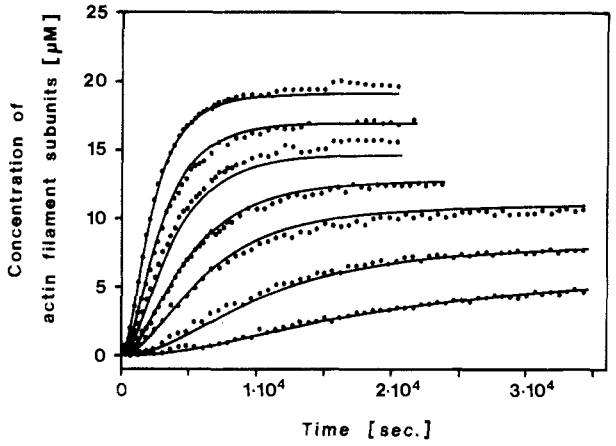

FIGURE 5: Polymerization kinetics of actin in the presence of 40 mM KCl. (···) Measured time course of polymerization; total actin concentrations 7.4, 9.6, 12.4, 14.2, 16.2, 18.4, and 20.5 μM. (—) Calculated curves using the parameters given in Table I.

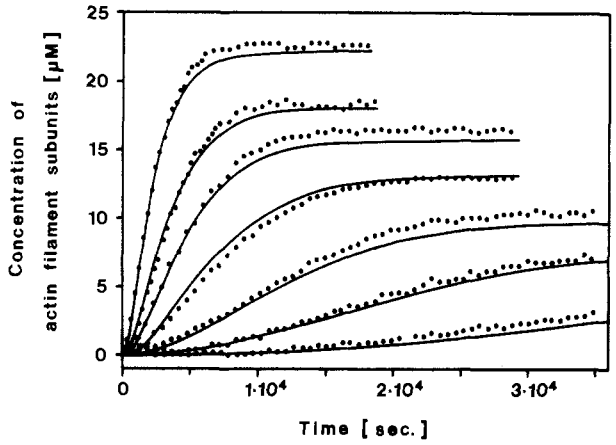

FIGURE 6: Polymerization kinetics of actin in the presence of 1.8 mM $CaCl_2$. (···) Measured time course of polymerization; total actin concentrations 6.9, 9.4, 11.7, 15.1, 17.7, 20.1, and 24.1 μM. (—) Calculated curves using the parameters given in Table I.

concentration on the total actin concentration is not caused by the presence of denatured nonpolymerizable actin. It remains unclear whether the observed increase of the monomer concentration with the total concentration is real or produced by the procedure of separating monomers and filaments. The critical concentrations obtained by the two methods were similar (Figures 2–4). For the quantitative analysis we used the values stemming from the centrifugation procedure because of the more accurate extrapolation (Table I).

Polymerization Kinetics of Actin. Figures 5–7 show the time dependence of the concentration of actin filament subunits ($C^* = c_{tot} - c_1$) under various conditions. The rate constants were fitted by seeking the smallest set of kinetic parameters necessary to reach a good agreement of the calculated curves with the measured curves. The ratio of the dissociation rate constant k' and the association rate constant k was obtained from the critical monomer concentration $\tilde{c}_1(\tilde{c}_1 = k'/k)$. The actin polymerization curves measured in the presence of potassium were found to be in good agreement with curves calculated for the assumption that monomers and trimers are in a fast preequilibrium; i.e., the rate of dissociation of dimers and trimers is fast compared to the rate of elongation of trimers to form tetramers ($k_2', k_3' \gg kc_1$). Calculated kinetic curves similar to the curves measured in the presence of calcium or magnesium could only be obtained when fragmentation of filaments was assumed to occur. The nucleus was treated as a labile tetramer ($k_2', k_3', k_4' \gg kc_1$). The rate constants

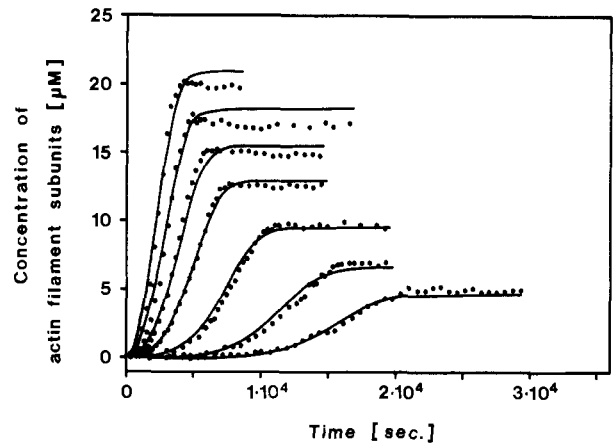

FIGURE 7: Polymerization kinetics of actin in the presence of 0.6 mM $MgCl_2$ and 0.5 mM EGTA. (···) Measured time course of polymerization; total actin concentrations 6.7, 8.5, 11.5, 14.9, 17.3, 20.3, and 22.9 μM. (—) Calculated curves using the parameters given in Table I.

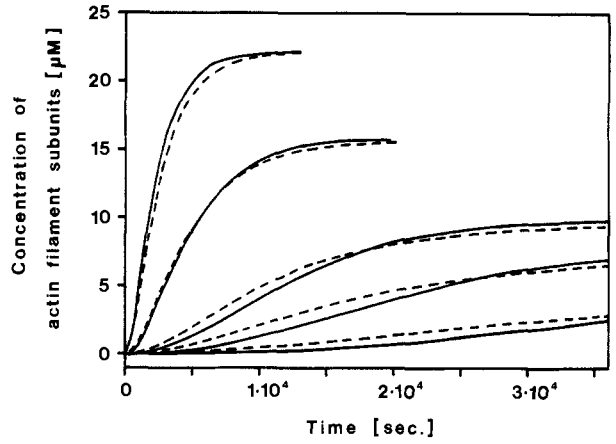

FIGURE 8: Calculated polymerization curves that are in best agreement with the curves measured in the presence of calcium; total actin concentrations 6.9, 9.4, 11.7, 17.7, and 24.1 μM. (---) Curves calculated for the assumption that no fragmentation occurs. The nucleus was treated as a labile trimer ($k'^2 \Pi_{i=2}^{i=3} (k_i/k_i') = 5.3\ M^{-2}\ s^{-2}$). (—) Curves calculated for the assumption that fragmentation occurs. Kinetic parameters are given in Table I.

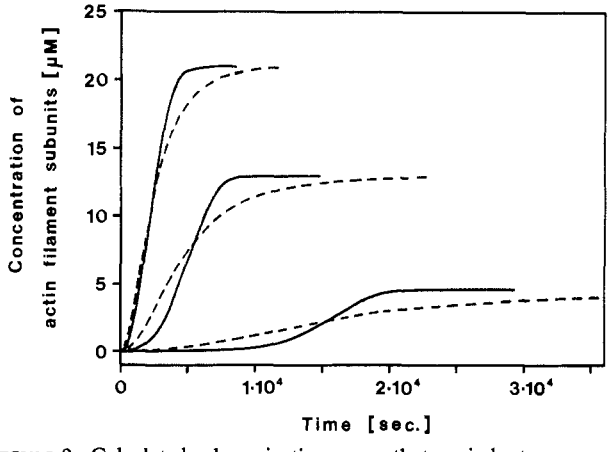

FIGURE 9: Calculated polymerization curves that are in best agreement with the curves measured in the presence of magnesium; total actin concentrations 6.7, 14.9, and 22.9 μM. (---) Curves calculated for the assumption that no fragmentation occurs. The nucleus was treated as a labile dimer ($k'^2(k_2/k_2') = 1.4 \times 10^{-4}\ M^{-1}\ s^{-2}$). (—) Curves calculated for the assumption that fragmentation occurs. Kinetic parameters are given in Table I.

available from this analysis are summarized in Table I (see eq 6 and 7).

So that the effect of fragmentation on the polymerization curves could be judged, the best fit from a mechanism without fragmentation was depicted in Figures 8 and 9 along with the curves calculated by taking into account fragmentation. Spontaneous fragmentation of filaments changes the shape of the polymerization curves significantly. On fragmentation of filaments, a long lag phase of polymerization is observed especially when the total concentration is near the critical monomer concentration (Figures 6–9). After nucleation of filaments, the self-reproduction by fragmentation leads to a fast increase of the number of filaments. This strongly increasing rate of filament formation causes a corresponding strongly increasing rate of monomer consumption which at the final stage of polymerization is compensated by dissociation of monomers from the filaments. On the other hand, when filaments are formed exclusively by nucleation, the rate of filament formation decreases continuously with the decreasing monomer concentration so that the monomer concentration approaches the final steady-state concentration slowly [e.g., polymerization in the presence of potassium (Figure 5)].

The shape of the measured polymerization curves can be explained by a simple model that takes into account nucleation, elongation, and fragmentation. Of course, this good agreement does not exclude the possibility that under the conditions applied in these experiments filaments associate end to end. However, it is impossible to interpret the polymerization curves by a model that includes nucleation, elongation, and end-to-end association but neglects fragmentation. Ferrone et al. (1980) have recently reported an investigation on the nucleation of sickle cell hemoglobin. They explained the long lag phase of sickle cell hemoglobin polymerization by a model in which nucleation was facilitated along the surface of existing polymers. An attempt to fit our data by this model was unsatisfactory because of the high concentration dependence of the nucleation rate. This alternative nucleation mechanism can be excluded by our results.

Discussion

Within the limits of the analysis presented in this study, one can estimate to what extent filaments are formed by nucleation and by fragmentation. The ratio r of the concentrations of filaments resulting from nucleation and fragmentation is given by (see eq 7)

$$r(t) = \left[\frac{k'^2 \prod_{i=2}^{i=n} (k_i/k_i')}{k' k_{ft}} \right] \left[\frac{\int_0^t (c_1/\bar{c}_1 - 1) c_1^n \, dt}{\int_0^t (c_{tot} - c_1) \, dt} \right] \quad (8)$$

At half-polymerization in the presence of calcium, nearly all filaments result from nucleation at the highest total actin concentration (24.1 μM) whereas about as many filaments result from nucleation as from fragmentation at the lowest total actin concentration (6.9 μM). On the other hand, at the highest total actin concentration in the magnesium experiment (22.9 μM), about equal numbers of filaments result from nucleation as from fragmentation, and nearly all filaments originate by fragmentation at the lowest total actin concentration (6.7 μM). The extent of fragmentation is qualitatively reflected by the magnitude of the deviation of the polymerization curves without fragmentation from the polymerization curves with fragmentation (Figures 8 and 9).

The experiments reported in this study provided evidence that actin may undergo spontaneous fragmentation and that the extent of fragmentation depends strongly on the experimental conditions. Whenever a protein or another molecule is found to cause formation of short filaments by capping one end of a filament, one should take into consideration the possibility that spontaneously broken filaments are prohibited from end-to-end reassociation by capping of the filament ends. An analysis of the type described in this paper may give insight to what extent spontaneous fragmentation occurs.

References

Brenner, S. L., & Korn, E. D. (1979) *J. Biol. Chem. 254*, 9982–9985.

Casassa, E. F. (1955) *J. Chem. Phys. 23*, 596–597.

Erickson, H. P., & Pantaloni, D. (1981) *Biophys. J. 34*, 293–309.

Ferrone, F. A., Hofrichter, J., Sunshine, H. R., & Eaton, W. A. (1980) *Biophys. J. 32*, 361–380.

Hasegawa, T., Takahashi, S., Hayashi, H., & Hatano, S. (1980) *Biochemistry 19*, 2677–2683.

Kawamura, M., & Maruyama, K. (1970) *J. Biochem. (Tokyo) 67*, 437–457.

Kondo, H., & Ishiwata, S. (1976) *J. Biochem. (Tokyo) 79*, 159–171.

Lusty, C. J., & Fasold, H. (1969) *Biochemistry 8*, 2933–2939.

MacLean-Fletcher, S., & Pollard, T. D. (1980) *Cell (Cambridge, Mass.) 20*, 329–341.

Nakaoka, Y., & Kasai, M. (1969) *J. Mol. Biol. 44*, 319–332.

Oosawa, F., & Kasai, M. (1962) *J. Mol. Biol. 4*, 10–21.

Pollard, T. D., & Mooseker, M. S. (1981) *J. Cell Biol. 88*, 654–659.

Rees, M. K., & Young, M. (1967) *J. Biol. Chem. 242*, 4449–4458.

Walsh, T. P., & Wegner, A. (1980) *Biochim. Biophys. Acta 626*, 79–87.

Wegner, A. (1976) *J. Mol. Biol. 108*, 139–150.

Wegner, A., & Engel, J. (1975) *Biophys. Chem. 3*, 215–225.